

Tartu University
Faculty of Science and Technology
Institute of Physics

Master Thesis

Model of a Self-Oscillating Ionic Polymer-Metal Composite Bending Actuator

Deivid Pugal

Supervisors: Prof. Kwang J. Kim
Heiki Kasemägi

Tartu 2008

Contents

List of Publications	2
1 Introduction	4
2 Overview	6
3 The Base Model	8
4 Self-Oscillations	14
4.1 Theoretical Background	14
4.2 Experiments	15
4.3 Modeling Self-Oscillations	17
4.4 Modeling Results	21
5 Summary and Conclusions	22
Acknowledgments	23
References	24
Ostsilleeruva IPMC aktuaatori mudel	27
PUBLICATIONS	29

List of Publications

CC and SPIE publications related to the thesis:

- I** D. Pugal, K. J. Kim, A. Punning, H. Kasemägi M. Kruusmaa, and A. Aabloo, “A self-oscillating ionic polymer-metal composite bending actuator,” *Journal of Applied Physics*, **103**, 084908, 2008
- II** D. Kim, K. J. Kim, Y. Tak, D. Pugal, and Il-S. Park, “Self-oscillating electroactive polymer actuator,” *Applied Physics Letters*, **90**, 184104, 2007
- III** D. Pugal, H. Kasemägi, K. J. Kim, M. Kruusmaa, and A. Aabloo, “Finite element simulations of the bending of the IPMC sheet,” in *Proceedings of International Society For Optical Engineering (SPIE)*, (EAPAD, San Diego, March 2007), pp 65240B

Publications not covered in the thesis:

- IV** D. Pugal, H. Kasemägi, M. Kruusmaa, and A. Aabloo, “An advanced finite element model of IPMC,” In *Proceedings of SPIE*, (EAPAD San Diego, March 2008), pp 692711
- V** M. Listak, D. Pugal, and M. Kruusmaa, “Biomimetic fish-like underwater robot for shallow water applications,” in *Proceedings of 13th International Conference on Advanced Robotics (ICAR)*, (Korea, Jeju, 21-24 August, 2007. IEEE, 2007), pp 332 - 336.
- VI** M. Listak, D. Pugal, and M. Kruusmaa, “Computational Fluid Dynamics Simulations of a Biomimetic Underwater Robot,” in *Proceedings of 13th ICAR* , (Korea, Jeju, 21-24 August, 2007. IEEE), pp 314 - 319.

- VII** M. Listak, G. Martin, D. Pugal, A. Aabloo, and M. Kruusmaa, “Design of a semi-autonomous biomimetic underwater vehicle for environmental monitoring,” in *Proceedings of 6th IEEE International Symposium on Computational Intelligence in Robotics and Automation*, (Espoo, Finland; 27.06.-30.06.2005. New York: IEEE, 2005), pp 9 - 14.

Chapter 1

Introduction

In the present thesis I consider simulations of ionic polymer-metal composite [1] (IPMC) type materials. IPMC is one of the types of electroactive polymers (EAP). EAPs include ferroelectric polymers [2], conducting polymers [3], carbon-nanotubes [4], dielectric elastomers [5], and ionic polymeric gels [6]. Given materials are valuable for a number of applications from micro robotics to military and space applications. The advantages of EAP materials are light weight, noiseless actuation, simple mechanics and large displacement. In addition some EAPs, such as IPMCs, are able to function in aqueous environments. Those qualities make the materials possible to use as artificial muscles.

IPMC materials are highly porous polymer materials like NafionTM, filled with a ionic conductive liquid. Water based IPMCs operate in aquatic environment and current is caused by ions such as Na^+ , K^+ dissociated in water. Ionic liquid based IPMCs do not need wet environment for operating. A sheet of an ionic polymer is coated with a thin metal layer, usually platinum or gold. All freely mobile cations inside the polymer migrate towards an electrode due to an applied electric field, causing expansion of the material at the one end of the sheet and contraction at the other end, which results in bending of the sheet.

Spontaneous oscillations are a widespread phenomenon in nature. They have been studied for large number of experiments, including electrochemical systems, such as the oxidation of metals and organic materials [7]. Electrochemical systems exhibiting instabilities often behave like activator-inhibitor systems. In these systems the electrode potential is an essential variable and takes on the role either of the activator or of the inhibitor. If

certain conditions are met, an activator-inhibitor system can generate oscillations [8]. A series of tests with IPMCs immersed in formaldehyde (HCHO) solution has been conducted by Kim et al. [9]. Measurements under constant electric field showed current oscillations and thus also material oscillations from onset potential of 0.75V.

In this thesis I give an short overview of different types of models used to simulate bending of an IPMC. Then I propose a general model for an IPMC. The model is extended to simulate electrochemical oscillations on the surface of an IPMC. The simulated data is validated against experimental data. The rest of the chapter at hand gives a brief introduction to IPMC oscillations and my model.

The primary goal of current work is to develop an extendable Finite Element model for simulating an IPMC muscle. The model consists of two parts - one is a base model which could be used for simulating simple deflection of an IPMC. The base model is based on physics, i.e. the underlying equations describe physical processes instead of being mere extrapolation of experimental data. There are only few Finite Element models developed for IPMC materials whereas it is possible to find rather many electromechanical models. One of the reasons could be that it is more difficult to relate experimental data to a model in case of Finite Element simulations. However, Finite Element Modeling (FEM) is very good for simulating coupled problems such as mass transfer, mechanics, electrochemistry, and etc, but it is generally not suitable for molecular scale simulations. Therefore the model couples macro scale equations of different domains such as Nernst-Planck equation for mass transfer and continuum mechanics equations to describe bending.

The second part of the model is an extension to the base model. It describes the electrochemical reactions and oscillating movement of an IPMC muscle. Therefore the second part of my model consists of four time-dependent differential equations, which describe the electrochemical reactions on the surface of an IPMC. The goal is to extend the base model to simulate a real experiment - a self-oscillating IPMC. Therefore the final model consists of the base model and electrochemistry model coupled together. The model is also validated against experimental data. The results of this thesis have also been published in Applied Physics Letters [9] and Journal of Applied Physics [10].

Chapter 2

Overview

There are several models available to describe tip displacement of an IPMC. For instance Newbury and Leo [11] proposed a linear model with mechanical terms - mechanical impedance and inertia, and two electric terms - DC resistance and charge storage. The model was based on an equivalent circuit representation that was related to the mechanical, electrical and electromechanical properties of the material. Expressions for the quasi-static and dynamic mechanical impedance were derived from beam theory. The electrical impedance was modeled as a series combination of resistive and capacitive elements. So the resulting linear electromechanical model was based on the measurement of the effective permittivity, elastic modulus, and effective strain coefficient.

There are more lumped models available. In those models input parameters such as voltage or current are converted to the output parameters - tip displacement, force, and etc. For instance Jung et al. modeled an IPMC as a high pass filter, using series of resistors and capacitors in their calculations [12]. The model was an equivalent electrical circuit model for the IPMC actuator using experimental data.

Punning proposed a non-linear transmission line model, where all the elements of transmission line had a physical meaning [13]. He showed that the IPMC model works as a delay line with changing resistors and the curvature of the IPMC sample at a given point depends on the surface resistance.

There are few Finite Element models for an IPMC available. Some authors like Nasser and Wallmersperger [14, 15] have already simulated mass transfer and electrostatic effects - similar approach is used in current thesis. Toi [16] proposed a Finite Element model, where viscosity terms in transportation processes were included explicitly. How-

ever, the basis of the described model was a rectangular beam with 2 pairs of electrodes. Instead of using continuum mechanical equations for simulating mechanical bending, analytical Euler beam theory is more commonly used by authors like Lee [17] and Wallmersperger [18].

As brought out in previous chapter, a series of tests with self-oscillating IPMCs were conducted by Kim et al. [9]. The initial oscillation model for an IPMC was proposed by D. Kim [19]. It was a numerical model, which was able to predict voltage and also tip displacement for certain experimental configuration. However the model was very rigid and did not work for different HCHO concentrations. The model was based on the work of Strasser [20], which is also the base of the electrochemical model proposed in this paper.

Chapter 3

The Base Model

An IPMC sheet consists of a polymer host and a metal coating. In our experiments, we have used NafionTM 117, coated with a thin layer of platinum. Mass transfer and electrostatic simulations are done in three mechanical domains - pure backbone polymer, pure platinum coating, and mixture of polymer and platinum - some platinum diffuses into the polymer during coating process [21]. Physical properties and dimensions of pure, 2 μm thick platinum coating are considered only when calculating bending. That gives us five mechanical domains as shown in Fig. 3.1. Most simulations are carried out for an IPMC strip, 2 – 4 cm long, 200 μm thick polymer, including 10 μm thick Pt diffusion region on each side, coated with 2 μm thick platinum, in a cantilever configuration - one end of the strip is fixed.

The Nernst-Planck equation describes diffusion, convection and in presence of electric field and charges, migration of the particles. The general form of the equation is

$$\frac{\partial C}{\partial t} + \nabla \cdot (-D\nabla C - z\mu FC\nabla\phi) = -\vec{u} \cdot \nabla C, \quad (3.1)$$

where C is concentration, D diffusion constant, F Faraday constant, \vec{u} velocity, z charge number, ϕ electric potential, and μ mobility of species, which is found by using known relation $\mu = D/(RT)$. There T is absolute temperature and R universal gas constant. Mobile counter ions are described by Eq. (3.1). As anions are fixed, they maintain constant charge density throughout the polymer. After a voltage is applied to the electrodes of an IPMC, all free cations will start migrating towards cathode, causing current in the outer electric circuit. Because of the fact that ions cannot move beyond the boundary of the polymer, charges start to accumulate, resulting in increase of the electric field, which

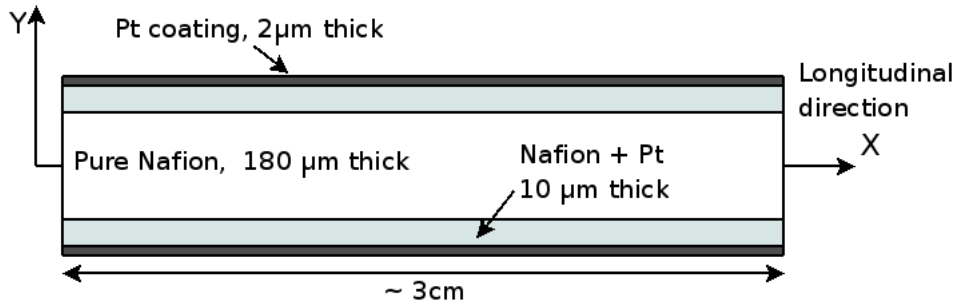


Figure 3.1: Illustration of domains and dimensions used in simulations. The length of 3 cm was used also in number of experiments. Notice that there are three different mechanical domains - pure NafionTM polymer, pure Pt coating and diffusion layer, where Pt has diffused into the polymer.

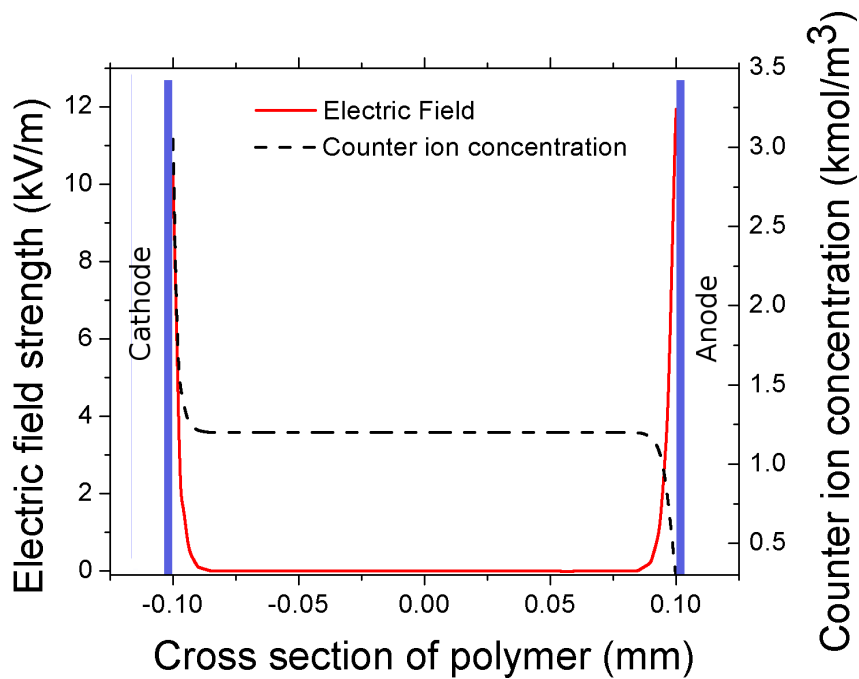


Figure 3.2: The concentration of counter ions and electric field strength inside the polymer according to simulations.

Table 3.1: Parameter values used in bending simulations.

Parameter	Value	Unit
D	1×10^{-6}	cm^2/s
R	8.31	$J/(K mol)$
T	293	K
z	1	—
F	96.5×10^6	mC/mol
ϵ	25	mF/m
A	110	$N m/mol$
B	10	$N m^4/mol^2$
$\alpha_{polymer}$	0	s^{-1}
$\beta_{polymer}$	1.5	s

cancels out the applied one. The process could be described by Gauss' Law:

$$\nabla \cdot \vec{E} = -\Delta\phi = \frac{F \cdot \rho_c}{\epsilon}, \quad (3.2)$$

where ρ_c is charge density, ϵ is absolute dielectric constant and E is the strength of the electric field. The charge density variable is related to charge concentration:

$$\rho_c = zC + z_{anion}C_{anion}. \quad (3.3)$$

The second term in Eq. (3.3) is constant at every point of the polymer. The coupling between equations (3.1) and (3.2) is strong, i.e. no weak constraints have been used. Absolute dielectric constant ϵ could be explicitly written as $\epsilon = \epsilon_0\epsilon_r$, where ϵ_0 is dielectric constant in vacuum and equals $8.85 \times 10^{-12} F/m$. The measured value of absolute dielectric constant ϵ is shown in Table 3.1. A steady state of the cations forms when electric field created by distribution of cations cancels out the applied electric field, i.e. the strength of the electric field inside the polymer is approximately zero, as also shown in Fig. 3.2. The steady state cation concentration, with average value of $1200 mol/m^3$ is also shown in the same figure. It is interesting to notice that there are fluctuations in charge distribution only in really thin boundary layers, leading to the conclusion that there is no charge imbalance inside the polymer. General understanding is that locally generated charge imbalance nearby platinum electrodes is directly connected, and mainly responsible, to the bending of an IPMC [22]. Therefore we define longitudinal force per

Table 3.3: Material parameters used in continuum mechanics equations.

Parameter	Value	Unit	Domain where applied
E_N	200	MPa	Nafion TM
ν_N	0.49	-	Nafion TM
E_{Pt}	168	GPa	Pt
ν_{Pt}	0.38	-	Pt
E_{diff}	84	GPa	Pt diffusion layer (estimated)
ν_{diff}	0.42	-	Pt diffusion layer (estimated)

unit area at each point in the polymer of an IPMC as follows [18]:

$$\vec{F} = (A \rho_c + B \rho_c^2) \hat{x}, \quad (3.4)$$

where ρ_c is charge density and A and B are constants which are found by fitting simulations according to experimental results using system identification. Values of the constants are brought out in Table 3.1 and it is interesting to notice that the ratio A/B is close to the value suggested by Wallmersperger [18]. Equations (3.1)-(3.4) are described only for pure NafionTM and Pt diffusion domain (see Fig. 3.1). There is no ion diffusion nor migration in thin Pt coating domain.

To relate the force in Eq. 3.4 to the physical bending of an IPMC sheet, we introduce a set of continuum mechanics equations, which are effective in all domains (Fig. 3.1). These equations are described in the Comsol Multiphysics structural mechanics software package. Normal and shear strain are defined as

$$\epsilon_i = \frac{\partial u_i}{\partial x_i}, \quad \epsilon_{ij} = \frac{1}{2} \left(\frac{\partial u_i}{\partial x_j} + \frac{\partial u_j}{\partial x_i} \right), \quad (3.5)$$

where u is the displacement vector, x denotes a coordinate and indices i and j are from 1 to 3 and denote components correspondingly to x , y , or z direction. The stress-strain relationship is

$$\sigma = D\epsilon, \quad (3.6)$$

where D is 6×6 elasticity matrix, consisting of components of Young's modulus and Poisson's ratio. The system is in equilibrium, if the relation

$$-\nabla \cdot \sigma = \vec{F}, \quad (3.7)$$

is satisfied. This is Navier's equation for displacement. The values of Young's modulus and Poisson's ratios, which are used in the simulations, are shown in Table 3.3. The values for platinum diffusion region are not measured, but estimated as an average of values of the pure NafionTM and Pt regions.

As our simulations are dynamic rather than static, we have to introduce an equation to describe the motion of an IPMC sheet. To do that, we use Newton's Second law

$$\rho \frac{\partial^2 \vec{u}}{\partial t^2} - \nabla \cdot c \nabla \vec{u} = \vec{F}, \quad (3.8)$$

where the second term is the static Navier's equation and c is Navier constant for static Navier's equation. The first term in Eq. (3.8) introduces the dynamic part. Several authors have reached to the conclusion that IPMC materials exhibit viscoelastic behavior [11, 23], which is especially noticeable for high frequency movements [24]. However, we include the viscoelastic term in our equations by means of using Rayleigh damping [25] model, which is described for a system of one degree of freedom as follows:

$$m \frac{d^2 u}{dt^2} + \xi \frac{du}{dt} + ku = f(t), \quad (3.9)$$

where the damping parameter ξ is expressed as $\xi = \alpha m + \beta k$. The parameter m is mass, k is stiffness and α and β are correspondingly damping coefficients. The equation for the multiple degrees of freedom is

$$\rho \frac{\partial^2 \vec{u}}{\partial t^2} - \nabla \cdot \left[c \nabla \vec{u} + c \beta \nabla \frac{\partial \vec{u}}{\partial t} \right] + \alpha \rho \frac{\partial \vec{u}}{\partial t} = \vec{F}. \quad (3.10)$$

By coupling Eq. (3.10) to the previously described equations, a good basic model for IPMC actuation has been obtained. The damping equation turned out to be very necessary to describe correct movement of an IPMC strip. Though the values of the parameters α and β are empirical (see Table 3.1), they have an important role of improving the dynamical behavior of the model for non-constant applied voltages.

All values, which are used in the simulations, have been brought out in Table 3.1. Fig. 3.3 shows a comparison between the simulation and an experiment [13]. More comparative figures are introduced in the next section of the paper.

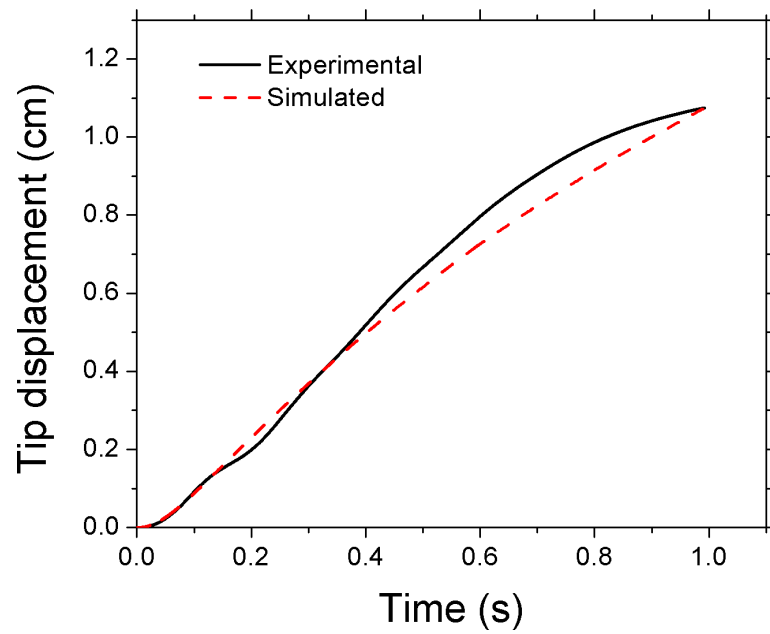


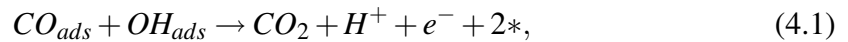
Figure 3.3: Experimental and simulation results of tip displacement. The simulation is done for potential of 2 volts. Although there is a slight difference of graphs in large displacement region, the model gives precise estimation for smaller displacement.

Chapter 4

Self-Oscillations

4.1 Theoretical Background

Studies show that there are sequential electrochemical reactions, which take place on the platinum cathode. The initial burst of the current is caused by the reaction



where subscript *ads* denotes species adsorbed to the platinum and * denotes an active platinum site. The result of the reaction (4.1) is clearing up 2 platinum sites, which causes *CO* to adsorb again. Due to *CO* poisoning, anodic current abruptly decreases until the burst again. Between current decrease and second burst, the current slightly increased due to *OH* adsorption. These electrochemical reactions lead to self-rhythmic motion of an IPMC as shown in Fig. 4.3. During the oxidation of formaldehyde, the intermediate (*CO*) of the reaction strongly binds to the platinum surface of the IPMC and blocks active sites. Since platinum is particularly vulnerable to a poisoning effect, both cathode and anode can be poisoned by *CO* in acidic media. In this process the resistance of platinum is increased which leads to weaker field strength between electrodes of an IPMC. Platinum also adsorbs *OH* which then oxidizes the *CO* on adjacent platinum sites to *CO*₂. Due to this reaction, conductivity of platinum improves and results in a stronger field strength between the electrodes. The simultaneous adsorption and desorption processes result in the oscillatory potentials which can be used as a driving source of IPMCs. Chronopotentiometry scans show that before reaction (4.1), the following

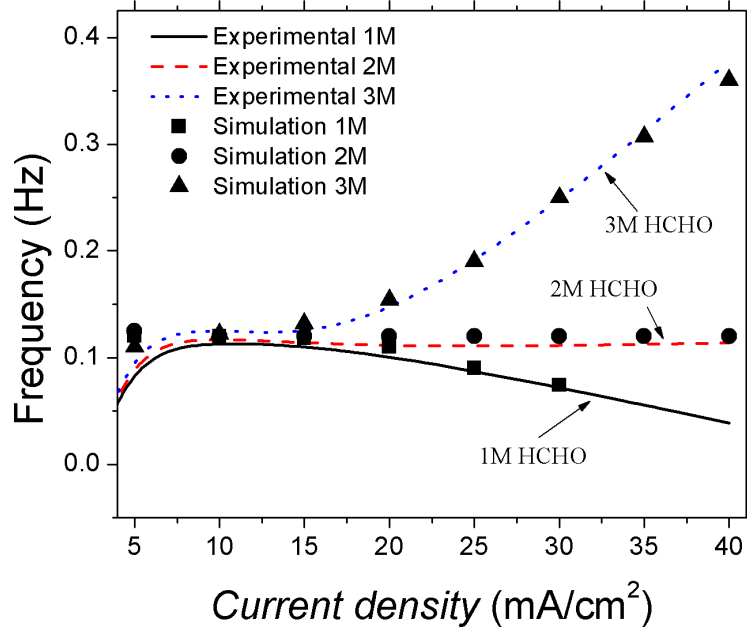
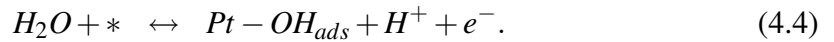
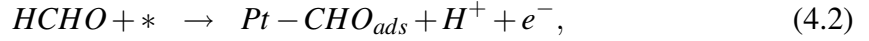


Figure 4.1: Experimental [9] and simulated frequency dependence on concentration of HCHO and applied current density. Simulations for 1 M HCHO concentration does not go past 30 mA/cm^2 , because given equation system did not give reasonable results beyond that current density.

reactions occur:



HCHO is dissociated on the electrode surface at lower anodic potentials. Higher anodic potentials cause dehydrogenation of water which results in water oxidation with intermediate Pt-OH formation. We believe that these reactions lead to oscillating potentials, which in turn lead to self-oscillating motion of the IPMC sheet.

4.2 Experiments

We have conducted a series of tests with IPMCs in a constant electric field in formaldehyde (HCHO) solution. Platinum-electroded IPMCs were prepared using the electroless deposition [26] onto Nafion 1110. The standard IPMC sample size was 0.27 mm thick \times

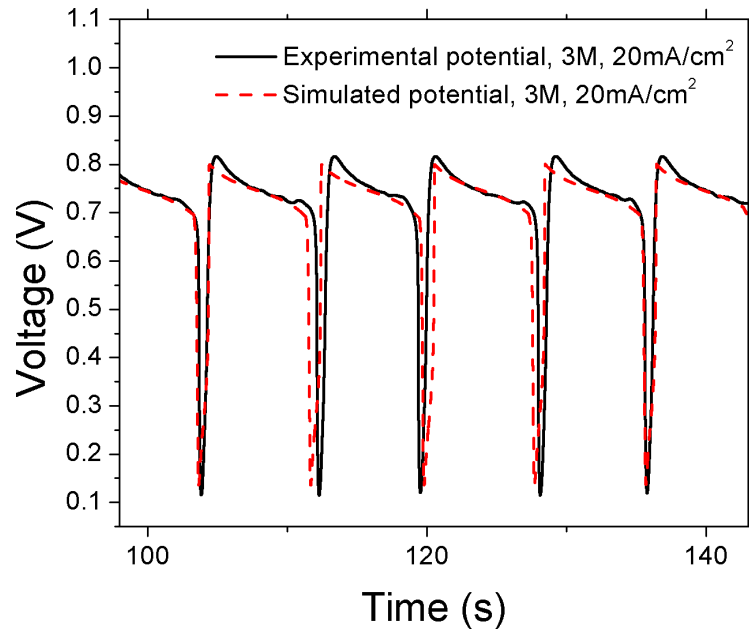


Figure 4.2: Potential oscillations. Measured data [19] and simulated data for 3 M HCHO solution. The potential oscillations were measured between the cathode and anode of the IPMC strip during the experiment. The applied current was maintained at constant value of 20 mA/cm^2 .

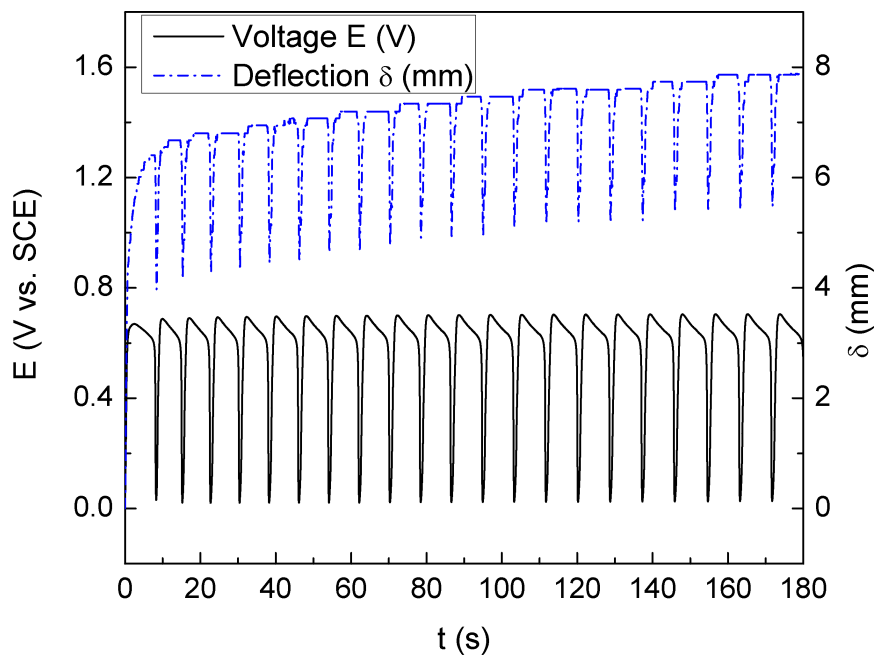


Figure 4.3: and corresponding deflection data of a platinum-IPMC in $2\text{MHCHO} + 3\text{MH}_2\text{SO}_4$ under constant current of 10mA/cm^2 (scan rate of 1mA/s).

10 mm wide \times 50 mm long. By using an INSTRONTM 5565, we measured the Young's modulus of the standard IPMC samples - 48.8 MPa. Actuation of the platinum electroded ionomer was carried out in a conventional electrochemical cell with three electrodes. The Reference Electrode (RE) used was a Saturated Calomel Electrode (SCE) and the two platinum electrodes functioned as the Working (WE) and Counter Electrode (CE), respectively. Voltammograms were obtained using a potentiostat/galvanostat (Radiometer Analytical, Voltalab80 Model PGZ402). Deformation data of IPMC in a cantilever configuration was obtained using a laser optical displacement sensor (Micro-Epsilon Model 1400-100). Prior to all experiments, dozens of cyclic voltammetric (CV) curves between $-0.25V$ and $+1.2V$ (vs. SCE) were performed in $0.5M H_2SO_4$ to confirm the absence of any residuals of impurities on the platinum surface. All experiments were performed at room temperature. Measurements show that current oscillations begin from applied potential of ca. $0.75 V$.

Series of chronopotentiometry scans were conducted to characterize oscillations for different HCHO concentrations and current densities. As was brought out in our previous paper [9], the oscillations start at approximately $7 mA/cm^2$. The experiments were conducted up to current density values of $40 mA/cm^2$. Tests with HCHO concentrations of $1 M$ (1 molar), $2 M$, and $3 M$ show that oscillations frequencies remain constant up to the current density of $14 mA/cm^2$, but after further increasing the current, in $1 M$ HCHO, the frequency decreases, in $2 M$ HCHO, the frequency remains constant, and in $3 M$ HCHO solution, the frequency starts to increase, as also shown in Fig. 4.1. More information about experiments and conclusions is described in the previous paper [9].

4.3 Modeling Self-Oscillations

Our goal is to develop a model for describing the frequency behavior depending on HCHO concentration and the current density. The basic model and concepts are introduced by D. Kim [19] and work of P. Strasser [20]. To describe the oscillations, four dynamic parameters, therefore four differential equations, must be observed: concentration of adsorbed OH , CO , the change of the double layer potential due to electrochemical reactions, and the change of the concentration of HCHO near the surface of platinum. First two variables are expressed for a certain current density and HCHO concentration

as [19]:

$$\dot{\theta}_{CO} = k_2M - k_4\theta_{CO}\theta_{OH}, \quad (4.5)$$

$$\dot{\theta}_{OH} = k_3\theta_{CO}M - k_{-3}\theta_{OH} - k_4\theta_{CO}\theta_{OH}, \quad (4.6)$$

where θ_{CO} and θ_{OH} are normed adsorption coverages of CO and OH. Variables k_i and M are described by equations

$$k_i(\phi) = \exp[s_i(\phi - \phi_i)], \quad (4.7)$$

$$M = (1 - \theta_{CO} - \theta_{OH}), \quad (4.8)$$

where s_i are modeling coefficients and ϕ_i are potentials of the reactions [19]. As our model is highly dynamic, the double layer with thickness δ near the platinum electrode is introduced. At the far end of the layer, the concentration of the formic acid is considered constant, and due to the adsorption of HCHO on Pt, the concentration of the solution is changing in time near the electrode. There are two components responsible of decrease of the concentration. The first one is direct oxidation of the formic acid to CO_2 and $2H^+$, the second one is adsorption of CO on the platinum surface due to electrochemical reactions [20]. The mechanism, which restores the HCHO concentration near the surface is diffusion. So the amount of the formic acid is decreasing significantly while the adsorption rate is high and increasing due to the diffusion during the low adsorption period. The equation describing the diffusion process is

$$\frac{\partial c_{FA}}{\partial t} = \nabla \cdot (D_{FA} \nabla c_{FA}) \quad (4.9)$$

with constant concentration at the far end of the double layer and flux

$$f = k_2M(1 + kc_r)S_{tot}, \quad (4.10)$$

as boundary condition on the electrode. Here S_{tot} denotes the total number of platinum sites per surface area, c_r is normed concentration near boundary layer and equals $c_r = c_{FA}/c_0$, where c_0 is an initial concentration. Variable k is a simulation constant. The second term of Eq. (4.10) represents simplified version of the direct oxidation path [20]. Considering those equations and interesting nature of frequency characteristic for different amounts of HCHO (Fig. 4.1), we can now describe empirical, gray box [27] equation

Table 4.1: Variables and values used in the simulation of electrochemical oscillations.

Parameter	Value	Unit
S_{tot}	0.5×10^{-6}	mol/cm^2
C_{dl}	1	mF/cm^2
A	1.2	$cm^7/(mA^2 \times mol)$
k	100	-
δ	3×10^{-2}	cm
D_{FA}	2.5×10^{-5}	cm^2/s
$\phi_{1,2,3,-3,4}$	[0.2, 0.3, 0.01, 0.512, 0.77]	V
$s_{1,2,3,-3,4}$	[10, -11, 9, -9, 20]	V^{-1}

for the last dynamic variable - the double layer potential:

$$\dot{\phi} = \frac{1}{C_{dl}} [j_{th} - j_d + A B j^2 (j - j_{th}) c_r - S_{tot} F (k_1 M + k_4 \theta_{CO} \theta_{OH})], \quad (4.11)$$

where j is applied current density, j_{th} is threshold current density with approximate value of $10 \text{ mA}/cm^2$, j_d is direct current density and is proportional to the second term of Eq. (4.10). The variable B is explicitly written as $B = c_0 - c_{neutral}$, where $c_{neutral}$ corresponds to concentration of 2 M . This is denoted as ‘‘natural’’ concentration, because as it is shown in Figure 4.1, the oscillation frequency for the case $c_0 = c_{neutral} = 2 \text{ M}$ does not depend on the applied current density. The numeric data can be found in Table 4.1. The third term in Eq. (4.11) is empirical and reflects the interesting behavior of the oscillations frequency for different formic acid concentrations. Other terms are similar to the ones described by Strasser [20]. However, some values are adjusted to get realistic simulation results. Measured voltage oscillation comparison to simulation data could be seen in Fig. 4.2. The simulation does not require any change in boundary or initial conditions for the basic model, which is described in the previous chapter. However, equations (4.5), (4.6), (4.7), and (4.11) are simulated using the weak form differential equation on the anode boundary.

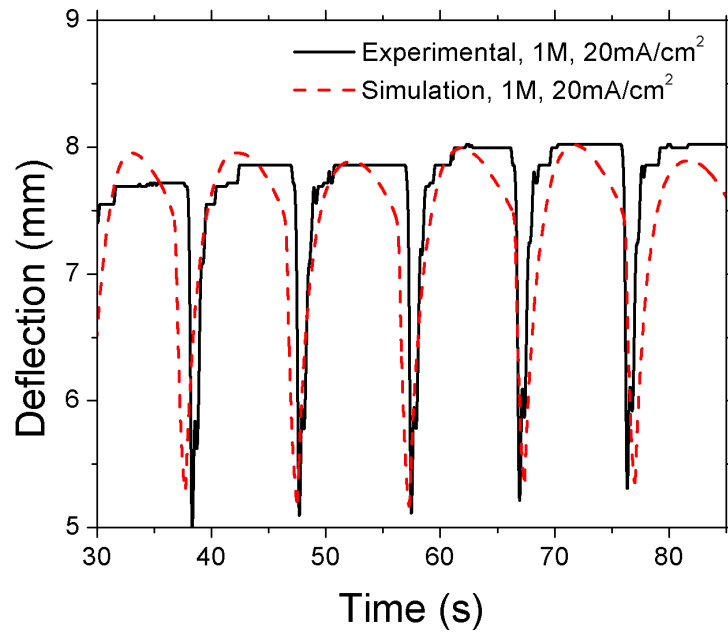


Figure 4.4: Oscillating tip displacement. Experimental [19] data and simulation data for 1 M HCHO solution, applied current density of 20 mA/cm^2 .

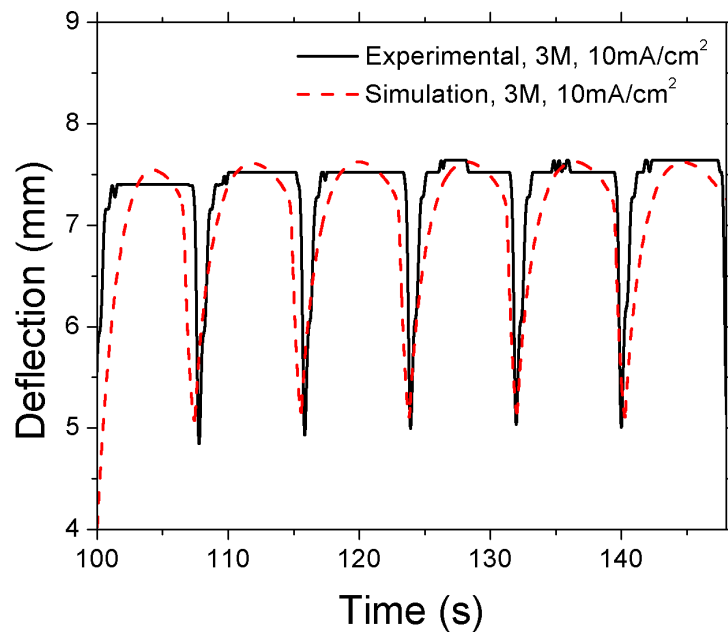


Figure 4.5: Oscillating tip displacement. Experimental [19] data and simulation data for 3 M HCHO solution, applied current density of 10 mA/cm^2 .

4.4 Modeling Results

By using the obtained voltage output in the base Finite Element Model, which is described in the previous chapter, we can simulate oscillating deflection of an IPMC muscle. As it is shown in Fig. 4.1, the model is quite flexible, i.e parameters such as HCHO concentration and current density could be changed without loss of model's accuracy. Also the measured voltage and modeled voltage is in very good accordance with modeling results (Fig. 4.2).

Two sample results for different HCHO concentrations and current densities are shown in Figures 4.4 and 4.5. As it could be seen, the amplitude, frequency and for the most part, shape of the deflection show reasonable agreement between modeling and experimental data. However, there is some disharmony at the areas of maximum deflection, where the experiments show distinctly sharp deflections in comparison to rather smooth simulation results. This will be studied further in future.

Chapter 5

Summary and Conclusions

We have developed a Finite Element model for simulating actuation of an IPMC. The model is largely based on physical quantities and well known or measurable variables. The migration and diffusion of the counter ions inside the NafionTM polymer is described along the electric field change due to the charge imbalance. This in turn is tied into continuum mechanics and dynamics equations, forming a complete system of equations to describe the bending of an IPMC sheet.

The comparison of experimental and simulated tip displacement in time shows reasonable agreement, especially for smaller deflections. The future work is to perform simulations more precise for large displacements, possibly including equations, which describe voltage distribution on the surface of the electrodes depending on the curvature of the IPMC. Taking into account the surrounding environment of the IPMC could also improve the results.

The second part of the work describes the extended model for self-oscillating IPMCs. The oscillations occur when a platinum coated IPMC is immersed into formic acid solution and subjected to a constant potential or current. The extended model takes into account formic acid concentration changes near the electrode and poisoning level of the platinum sites. This in turn results in the oscillating double layer potential, which is used in the base model for calculating time dependent tip displacement of the IPMC muscle. For the most part, the model follows simulation data closely. However, the experimental deflection shows distinctly sharp movements at certain regions, but the simulation gives rather smooth displacement profiles. The future work includes studying further this interesting behavior and possibly improving the model.

Acknowledgments

I want to acknowledge the support of the US Office of Naval Research (N00014-04-0673) and Estonian Science Foundation grant #6763. Also I acknowledge Estonian Archimedes Foundation for travel support of Deivid Pugal to University of Nevada, Reno. I want to thank my supervisors Kwang J. Kim (University of Nevada, Reno) and Heiki Kasemägi (Tartu University). I also thank my wife Kersti for her support.

References

- [1] M. Shahinpoor and K. J. Kim, “Ionic polymer-metal composites: I. fundamentals,” *Smart Materials and Structures* **10**, pp. 819–833, Aug. 2001.
- [2] Q. Zhang, V. Bharti, and X. Zhao, “Giant Electrostriction and Relaxor Ferroelectric Behavior in Electron-Irradiated Poly (vinylidene fluoride-trifluoroethylene) Copolymer,” *Science* **280**(5372), p. 2101, 1998.
- [3] E. I. Smela, “Conjugated polymer micromuscles,” *MST News*, pp. 16–18, Sept. 2003.
- [4] R. H. Baughman, C. Cui, A. A. Zakhidov, Z. Iqbal, J. N. Barisci, G. M. Spinks, G. G. Wallace, A. Mazzoldi, D. De Rossi, A. G. Rinzler, O. Jaschinski, S. Roth, and M. Kertesz, “Carbon nanotube actuators,” *Science* **284**, pp. 1340–4, May 21.
- [5] R. Pelrine, R. Kornbluh, Q. Pei, and J. Joseph, “High-speed electrically actuated elastomers with strain greater than 100%,” *Science* **287**, pp. 836–9, Feb. 4.
- [6] S. J. Kim, G. M. Spinks, S. Prosser, P. G. Whitten, G. G. Wallace, and S. I. Kim, “Surprising shrinkage of expanding gels under an external load,” *Nature Materials* **5**, pp. 48–51, Jan. 2006.
- [7] B. Miller and A. Chen, “Oscillatory instabilities during the electrochemical oxidation of sulfide on a Pt electrode,” *Journal of Electroanalytical Chemistry* **588**, pp. 314–323, Mar. 2006.
- [8] K. Krischer, “Spontaneous formation of spatiotemporal patterns at the electrode | electrolyte interface,” *Journal of Electroanalytical Chemistry* **501**, pp. 1–21, Mar. 2001.

- [9] D. Kim, K. J. Kim, Y. Tak, D. Pugal, and I.-S. Park, "Self-oscillating electroactive polymer actuator," *Applied Physics Letters* **90**(18), p. 184104, 2007.
- [10] D. Pugal, K. J. Kim, A. Punning, H. Kasemagi, M. Kruusmaa, and A. Aabloo, "A self-oscillating ionic polymer-metal composite bending actuator," *Journal of Applied Physics* **103**(8), p. 084908, 2008.
- [11] K. M. Newbury and D. J. Leo, "Linear electromechanical model of ionic polymer transducers - part i: Model development," *Journal of Intelligent Material Systems and Structures* **14**, pp. 333–342, June 2003.
- [12] K. Jung, J. Nam, and H. Choi, "Investigations on actuation characteristics of IPMC artificial muscle actuator," *Sensors and Actuators A (Physical)* **107**, pp. 183–92, Oct. 15.
- [13] A. Punning, M. Kruusmaa, and A. Aabloo, "Surface resistance experiments with IPMC sensors and actuators," *Sensors and Actuators, A: Physical* **133**, pp. 200–209, Jan. 2007.
- [14] S. Nemat-Nasser and S. Zamani, "Modeling of electrochemomechanical response of ionic polymer-metal composites with various solvents," *Journal of Applied Physics* **100**(6), p. 064310, 2006.
- [15] T. Wallmersperger, B. Kroplin, and R. W. Gulch, "Coupled chemo-electromechanical formulation for ionic polymer gels - numerical and experimental investigations," *Mechanics of Materials* **36**, pp. 411–420, May 2004.
- [16] Y. Toi and S.-S. Kang, "Finite element analysis of two-dimensional electrochemical-mechanical response of ionic conducting polymer-metal composite beams," *Computers and Structures* **83**, pp. 2573–2583, Dec. 2005.
- [17] S. Lee, H. C. Park, and K. J. Kim, "Equivalent modeling for ionic polymer - metal composite actuators based on beam theories," *Smart Materials and Structures* **14**, pp. 1363–1368, Dec. 2005.
- [18] T. Wallmersperger, D. J. Leo, and C. S. Kothera, "Transport modeling in ionomeric polymer transducers and its relationship to electromechanical coupling," *Journal of Applied Physics* **101**(2), p. 024912, 2007.

- [19] D. Kim, *Electrochemically Controllable Biomimetic Actuator*. PhD thesis, University of Nevada, Reno, USA, 2006.
- [20] P. Strasser, M. Eiswirth, and G. Ertl, "Oscillatory instabilities during formic acid oxidation on pt(100), pt(110) and pt(111) under potentiostatic control. II. model calculations," *Journal of Chemical Physics* **107**, July 1997.
- [21] S. Nemat-Nasser and Y. Wu, "Comparative experimental study of ionic polymer-metal composites with different backbone ionomers and in various cation forms," *Journal of Applied Physics* **93**, pp. 5255–5267, May 2003.
- [22] S. Nemat-Nasser and J. Y. Li, "Electromechanical response of ionic polymer-metal composites," *Journal of Applied Physics* **87**, Apr. 2000.
- [23] K. Yagasaki and H. Tamagawa, "Experimental estimate of viscoelastic properties for ionic polymer-metal composites," *Physical Review E - Statistical, Nonlinear, and Soft Matter Physics* **70**, pp. 052801–1, Nov. 2004.
- [24] K. M. Newbury and D. J. Leo, "Linear electromechanical model of ionic polymer transducers - part II: Experimental validation," *Journal of Intelligent Material Systems and Structures* **14**, pp. 343–358, June 2003.
- [25] R. Lord, "The Theory of Sound," *New York, Dover* **2**, p. 226, 1945.
- [26] K. Kim and M. Shahinpoor, "Ionic polymer-metal composites: II. Manufacturing techniques.," *Smart Materials and Structures* **12**(1), pp. 65–79, 2003.
- [27] M. Shahinpoor and K. J. Kim, "Ionic polymer-metal composites: III. modeling and simulation as biomimetic sensors, actuators, transducers, and artificial muscles," *Smart Materials and Structures* **13**, pp. 1362–1388, Dec. 2004.

Ostsilleeruva IPMC Aktuaatori Mudel

Deivid Pugal

Kokkuvõte

Käesolevas töös on koostatud IPMC (*ionic polymer-metal composite*) tüüpi materjalide mudel. IPMC on üks paljudest elektroaktiivsetest polümeeridest nagu ferroelektrilised polümeerid, juhtivad polümeerid, dielektrilised elastomeerid ja ioonpolümeer geelid. Kõik need materjalid on väärtuslikud paljudes rakendustes mikrobootikast kosmosetehnoloogiateni. Seda liiki materjalide eeliseks on kergus, hääletu töö ja suur paindeulatus. Mitmed elektroaktiivsed polümeerid, kaasa arvatud IPMC on võimelised toimima ka märjas keskkonnas. Neid omadusi silmas pidades võib kõiki eelnimetatud materjale kutsuda n.ö kunstlihasteks.

Käesolevas töös on koostatud IPMC tüüpi materjali jaoks füüsikaline mudel lõplike elementide meetodit (LEM) kasutades. Mudel koosneb kahest komponendist: üks ja põhiline on baasmudel, mille abil on võimalik simuleerida lihtsat IPMC materjali paindumist. See komponent sisaldab endas IPMC sees toimuvaid põhilisi protsesse (nagu ionide liikumine, elektrivälja kirjeldus) kirjeldavaid võrrandeid. Teine osa mudelist keskendub elektrokeemiliste protsesside kirjeldamisele ning see võimaldab simuleerida iseostsilleeruvat IPMC materjali. Nimelt on tehtud arvukalt teste IPMC materjalidega, mis on kastetud HCHO lahusesse. Rakendades materjalile konstantse pinget, alates 0.75V, saab mõõta voolu ja ka materjali enda võnkumisi. Seega mudeli teine osa ongi baasmudeli üks võimalik laiendus, mille abil saame modelleerida reaalselt füüsiliselt huvipakkuvat probleemi.

Baasmudeli võrrandid kirjeldavad mitut erinevat füüsikalist domeeni: Nernst Planck'i võrrand ionide liikumist, Gaussi võrrand elektrivälja IPMC materjalis ja mitmesugused

pideva keskkonna mehhaanika võrrandid ($\sigma - \varepsilon$ seosed) kirjeldavad materjali paindumist. Mudeliga sooritatud arvutuste ja katseandmete võrdlemine näitab head kooskõla.

Mudeli teine osa on sisuliselt baasmudeli laiendus elekrokeemiliste ostsillatsioonide kirjeldamiseks. See koosneb neljast süsteemi pandud ajast sõltuvast differentiaalvõrrandist, mis kirjeldavad mitmesuguseid elekrokeemilisi protsesse plaatinakatoodi pinnal. Võrrandite muutujateks on *HCHO* kontsentratsiooni katoodi lähedal, *CO* ja *OH* adsorptsioon ajas ja kaksikkihi potentsiaali muutumine ajas. Need võrrandid on samuti koostatud käesoleva töö raames.

Võrreldes nii baasmudeli kui ka laiendatud mudeli abil arvutatud IPMC tüüpi materjalide paindumist elektriväljas katseandmetega, näeme väga head kooskõla. Siiski eksperiment *HCHO* lahuses asetseva kunstlihasega näitab mõningaid järske liikumisi erinevalt meie mudelist. Selle huvitava käitumise uurimine on edaspidise uurimistöö osa.

Käesolevas töös esitatud tulemused on ka avaldatud ajakirjades *Applied Physics Letters* [9] ja *Journal of Applied Physics* [10].

PUBLICATIONS

I - Applied Physics Letters

<http://dx.doi.org/10.1063/1.2735931>

II - Journal of Applied Physics

<http://dx.doi.org/10.1117/12.776610>